New Journal of Physics
The open–access journal for physics

Exchange interaction effects in NO core-level photoionization cross-sections

A Rüdel[1], U Hergenhahn[2,4], K Maier[1], E E Rennie[1,5], O Kugeler[1,6], J Viefhaus[1], P Lin[3], R R Lucchese[3] and A M Bradshaw[2]

[1] Fritz-Haber-Institut der Max-Planck-Gesellschaft, Faradayweg 4-6, 14195 Berlin, Germany
[2] Max-Planck-Institut für Plasmaphysik, EURATOM association, Boltzmannstraße 2, 85748 Garching, Germany
[3] Department of Chemistry, Texas A&M University, Box 30012, College Station, TX 77842-3012, USA
E-mail: uwe.hergenhahn@ipp.mpg.de

New Journal of Physics **7** (2005) 189
Received 8 June 2005
Published 6 September 2005
Online at http://www.njp.org/
doi:10.1088/1367-2630/7/1/189

Abstract. The effect of the exchange interaction in the photoionization continuum is investigated, using N 1s photoionization of NO into the $1s^{-1}2\pi$ ($^1\Pi$) and ($^3\Pi$) final states as an example. The separation in energy of these two final states is 1.41 eV. Significant differences in their partial photoionization cross-sections are observed over a wide range of energies and cannot be accounted for by the different multiplicity of the states. We suggest that the deviation of the $^3\Pi/^1\Pi$ cross-section ratio from the statistical weighting at intermediate energies is dominated by the difference in the final-state potential experienced by the photoelectron and at asymptotically high energies by the multiplet-dependent amount of intensity going into multi-electron (shake-up) processes. Calculations underpinning this point are presented. We also show supporting measurements of the $^3\Pi/^1\Pi$ cross-section ratio for O 1s ionization and the absolute photoabsorption cross-section for NO over a wide energy range covering the core level region.

[4] Author to whom any correspondence should be addressed.
[5] Present address: Chemistry Department, University of Ottawa, Canada K1N 6N5.
[6] Present address: BESSY mbH, Albert-Einstein-Str. 15, 12489 Berlin, Germany.

PII: S1367-2630(05)01448-5

Contents

1. Introduction

One hundred years after Einstein's introduction of the concept of the photon in order to explain the photoelectric effect [1], photoionization experiments with an astounding degree of sophistication are possible. For isolated molecules, experiments can be performed, which probe the energy distribution and spatial distribution of photoelectrons from a fixed-in-space molecule. This can be achieved by aligning the molecule with a laser pulse [2, 3], or by determining the molecular axis direction in retrospect by detection of one or several ionic fragments, e.g. [4]–[14]. From these experiments, in a number of cases the full quantum mechanical transition matrix for the photoionization process has been extracted (e.g. [12], [15]–[18]).

To interpret experiments at this level of detail, the mechanisms which have to be taken into account for the formation of the photoelectron single-particle wavefunction have to be known precisely. Although the photoelectron is asymptotically free, in the molecular region it is still part of a multi-electron system with a total wavefunction which has to be properly antisymmetrized. For bound systems, antisymmetrization of the multi-electron wavefunction leads to energy differences between states with identical electronic configuration, but different spin coupling. This is often described as the consequence of an exchange interaction. In the photoionization of open-shell systems, exchange interactions between the bound electrons will lead to energy differences between the final ionic states. However, the extent to which the exchange interaction between bound electrons and the outgoing photoelectron affects the ionization process is not easily accessible.

In this paper, we report partial cross-section data for photoionization of the N 1s electrons in nitric oxide (NO) up to a kinetic energy of 600 eV and compare the results with calculations. Due to its valence, electronic configuration of $3\sigma^2 4\sigma^2 1\pi^4 5\sigma^2 2\pi^1$ NO is an open-shell molecule, in which core-level photoionization can lead to two channels differing by the spin coupling within the remaining ion: NO N $1s^{-1}2\pi$ ($^1\Pi$) and N $1s^{-1}2\pi$ ($^3\Pi$). These two ionic states create scattering potentials for the outgoing photoelectron, which differ in the exchange interaction that the photoelectron experiences while leaving the molecular ion. We show that the partial cross-sections pertaining to the two channels behave differently over a wide range of photoelectron energies. Since for a molecule as light as NO, the spin–orbit coupling is very small, this represents a clear example of the influence of the exchange interaction on the photoionization process.

The basic features of the N 1s photoelectron spectrum of NO are known from investigations with a Mg Kα X-ray source by Bagus *et al* [19]. These authors were able to resolve the energy difference between the singlet and triplet ionic state and found an intensity ratio of the singlet to triplet lines of 1 : 3.43(8) at a photon energy of 1.254 keV, which differs significantly from the expected statistical value of 1 : 3. This was attributed to different amounts of relaxation in the two ionic states. Assuming that the dipole matrix element is identical for the two states at high energies, their intensity ratio in a photoelectron spectrum depends, apart from the degeneracy factor, on the overlap between the valence orbitals in the initial and final state. Due to relaxation, this factor is generally less than unity, which leads to a reduction of the main line intensity and a proportionate appearance of shake-up satellites. Its quantitative dependence on the ionic state was reproduced by a calculation of Darko *et al* [20].

Further data on the inner-shell photoionization of NO was obtained in an early photon energy-dependent experiment, but the separation of the two exchange-split ionic states was not possible [21]. Subsequent investigations concentrated on the shape resonance region. Symmetry-resolved ion yield spectroscopy yielded shape resonance positions very close to the ionization thresholds of the N and O K-shells [22]. In the σ-channel of the ion yield, at the N K-edge a double structure of the resonance was observed, which was interpreted with the aid of spin-state resolved photoelectron spectra as a first maximum due to double excitations, followed by a single-shape resonance, which can decay in both the $^3\Pi$ and $^1\Pi$ channel [23]. The same group has investigated the partial wave composition of the outgoing N 1s wavefunction by photoelectron spectroscopy from NO molecules with selected spatial-axis directions [24].

In this paper, we will first present and discuss our results for the NO N 1s photoionization of NO. Subsequently, some results for the O 1s edge will be presented.

2. Experiment

Experimental results were obtained at several runs at the synchrotron radiation facilities NSLS (Brookhaven, USA), HASYLAB (Hamburg, Germany) and BESSY (Berlin, Germany). The bulk of the photoelectron spectra were taken on the X1B undulator beamline at the NSLS [25], using a stationary, magic angle cylindrical mirror analyser (CMA), the axis of which is collinear with the incoming synchrotron radiation beam [26]. A rotationally symmetric slit around the interaction region served as the gas inlet. The instrument is equipped with a cylindrically symmetric entrance lens and therefore can be operated in constant pass energy mode. Two different series of NO N 1s main line spectra were recorded with pass energies of 15 eV and 30 eV, giving an electron energy resolution of 95–135 meV and 195–290 meV, respectively, depending on the electron kinetic energy. The photon energy resolution for the two series was set to 80 and 200–320 meV, respectively. A series of NO O 1s main line spectra was recorded with a pass energy of 15 eV and a photon energy resolution of 200–240 meV. All spectra taken with this setup were normalized to the intensity of the incident light by alternate measurements of either the Ne 2p photoelectron line (N 1s spectra) or the Ar 2p photoelectron line (O 1s spectra) [27]. The transmission function of the analyser has been determined earlier [28] and was used to normalize the data. At HASYLAB, an electron time-of-flight (TOF) analyser, similar to the one described in [29], was used under the quasi-magic angle in a plane perpendicular to the light propagation axis. In this setup, the target gas entered the interaction region through a thin needle ($\varnothing = 220\ \mu$m) also mounted perpendicular to the photon beam. The spectra were obtained

on the BW3 undulator beamline with 350–460 meV total experimental resolution, depending on the photon energy [30]. For the time-to-energy conversion of the TOF-spectra the known kinetic energy positions of the NO-KLL Auger lines [31] have been used as well as the NO N 1s main line [32]. Finally, some high-resolution spectra were recorded at the undulator beam line U49/1-SGM [33] of the third generation synchrotron radiation source BESSY. Here, a hemispherical analyser (Scienta ES-200 [34]) was used, again mounted within the dipole plane under the quasimagic angle. At a pass energy of 10 eV a total experimental resolution of 67 meV for the N 1s spectrum was achieved. For the O 1s spectrum, the settings were 20 eV pass energy and 90 meV total experimental resolution. The ionization volume was enclosed by a stainless steel gas cell, which included a photoelectron dump to prevent backscattered electrons from entering the analyser and electrodes to apply a compensation voltage along the light axis passing through the sample volume [35]. The photon energy scale was calibrated using results from electron energy loss spectroscopy (EELS) measurements for NO N 1s $\rightarrow \pi^*$, $^2\Sigma^-$ $v' = 0$ at $h\nu = 399.67$ eV [32] and—in the case of the experiment at BESSY II—N_2 N 1s $\rightarrow \pi^*$, $1\sigma_u \rightarrow 1\pi_g$, $v' = 0$ at $h\nu = 400.88$ eV [36]. In all experiments, the synchrotron radiation was linearly polarized with the electric field vector directed along the horizontal. Components of the gas inlet system were made of corrosion resistant substances, such as stainless steel and PTFE and the system was flushed with an inert gas repeatedly before and after letting in NO.

All spectra were subjected to a least squares fit to determine the spectroscopical quantities of interest. We included vibrational excitations up to $v' = 3$ for each of the two multiplet lines. For the line shape, we have used a Lorentzian form distorted by Post-Collision-Interaction (PCI). An analytical parametrization of the resulting profile derived by Kuchiev and Sheinerman was chosen [37, 38]. For each of the two multiplet states, one vibrational progression was modelled by a coupling constant a, from which the intensities of all vibrationally excited states v' were derived with the aid of the linear coupling approximation: $p(v') = \exp(-a)\, a^{v'}/v'!$ [39]. The vibrational levels were assumed to be equidistant in energy. The resulting curves were convoluted by a Gaussian to account for experimental broadening. For the spectra taken with the CMA, the empirically determined analyser transmission profile was also convoluted with the calculated profile [40].

The absolute photoabsorption cross-section of NO was measured with a gas cell employing Si : N windows [41]. The cross-section was extracted from measurements of the photocurrent in front and behind of the cell, using a scan with an evacuated cell and otherwise identical parameters for normalization. Measurements were carried out at the HE-TGM1 beamline of the synchrotron radiation source BESSY I, predecessor of the current BESSY facility. The influence of higher order radiation has been suppressed by an arrangement of two grazing incidence mirrors. Further information on the apparatus has been published [42]. In order to subtract the valence contribution to the cross-section in the core-level region, we have approximated its influence by fitting a power law to a portion of the cross-section at photon energies below the first K-shell resonance and subtracting the resulting curve at all photon energies. Absolute cross-sections shown in this work include this correction.

3. Theory

Theoretical results were obtained by first performing a multiconfiguration self-consistent-field (MCSCF) calculation on the ion ground state of NO^+ using all core and valence orbitals. The natural orbitals were then used in CI calculations for both neutral and ion states and

in multichannel Schwinger configuration interaction (MCSCI) calculations [43]–[45]. The maximum l used for the expansion of the bound and continuum orbitals was 60 and in the asymptotic region it was 18. At the experimental ground state equilibrium bond distance of 1.1508 Å [46], the ionization potentials were 409.59 and 410.44 eV for the $^3\Pi$ and $^1\Pi$ states, respectively. We have performed two-channel MCSCI calculations of the transition matrix elements for the N 1s photoionization of NO molecules leading to the $^3\Pi$ and $^1\Pi$ final states at bond distances R of 1.0508, 1.1008, 1.1508, 1.2008 and 1.2508 Å.

Calculated values of the energy difference between the $^1\Pi$ and the $^3\Pi$ potential curve at these bond lengths are somewhat lower than the observed adiabatic exchange splitting (see below). Their trend shows a decrease from 0.9655 eV over 0.9079, 0.8494, 0.7882 to 0.7224 eV with increasing bond distance, which shows that the N–O bond in the NO^+ N $1s^{-1}$ $^1\Pi$ state undergoes slightly less shortening than in the $^3\Pi$ state. This agrees with the findings in earlier calculations [47] and with the observation of a larger degree of vibrational excitation in the $^3\Pi$ than in the $^1\Pi$ state at photon energies away from the threshold region [48].

The partial cross-sections were very rapidly varying functions of the internuclear coordinate R, so that intermediate values could not be interpolated by standard spline or polynomial functions. Thus, we fit each partial cross-section to a Fano profile, the parameters of which were found to be well approximated by quadratic polynomials in R. Vibrationally specific partial cross-sections were obtained by integrating over R the product of the R-dependent Fano profiles, the initial ground state and the final-state vibrational wavefunctions. Vibrationally averaged cross-sections were then obtained by a summation of the vibrationally specific cross-sections to all final ion vibrational states. Averaging over the vibrational motion had a significant effect in the region of shape resonance near the threshold. At energies above 50 eV kinetic energy, we give cross-sections that were computed with the bond length fixed at $R = 1.1508$ Å. As a consequence, the calculations for the partial cross-section have a discontinuity in the order of 1% at 50 eV kinetic energy.

4. Results: NO N 1s

The high resolution N 1s photoelectron spectrum of NO, recorded at BESSY, is shown in figure 1. The splitting of the main line into two components corresponding to triplet and singlet spin coupling can easily be resolved. Its value is 1.41 eV. This exchange effect is purely dependent on the ionic states and the magnitude of the splitting does not vary with photon energy. The vibrational fine-structure of the two lines is also well resolved and a vibrational energy of 237(5) meV was determined within the harmonic approximation for both lines. The ionization potentials of the N $1s^{-1}2\pi(^3\Pi)$ and $(^1\Pi)$ states were found at 410.34 and 411.81(2) eV by extrapolation of the pre-edge Rydberg series [32], and at 410.32(4) and 411.68(13) eV by photoelectron spectroscopy with an x-ray line source [49]. These give exchange splittings of 1.36 and 1.47 eV, respectively. Our value lies in between these previous measurements.

We have measured the cross-section for ionization into the $^3\Pi$ and the $^1\Pi$ final states over a wide range of energies. The sum of both components is displayed on an absolute scale in figure 2. We arrived at this figure by scaling the low-energy data of our work and the literature data by Lindle *et al* [21] to coincide with the maximum of the absorption curve at 415.4 eV. At this low energy, contributions of N 1s photoelectron satellites to the total absorption cross-section are not expected. Implicitly, we also assume that the total photoabsorption cross-section at its maximum is not influenced by neutral double excitations that decay to other channels than the N 1s main

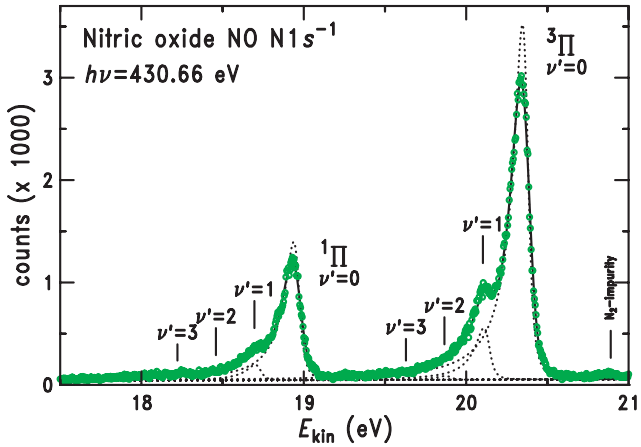

Figure 1. The NO N 1s main line photoelectron spectrum, showing the ionic $^3\Pi$ and $^1\Pi$ states split by the exchange interaction. Circles: experiment; solid line: least-squares fit; dashed lines: vibrational components of the fit, not convoluted with the apparatus function.

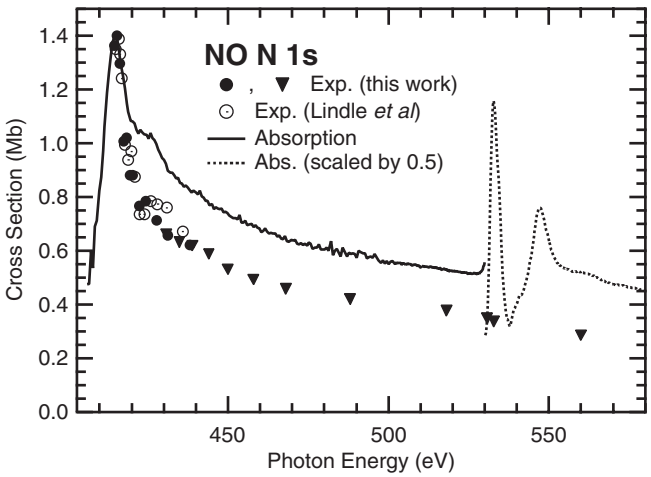

Figure 2. Intensity of the NO N 1s photoelectron main lines, sum of both multiplet components. Open circles are from Lindle *et al* [21]. All data sets were scaled to coincide with the absolute photoabsorption cross-section at its maximum at 415.4 eV. The valence contribution to the cross-section was subtracted beforehand, as explained in the experimental section.

line. As the sum of our N 1s single-hole and satellite cross-sections at higher photon energy is again consistent with the total absorption data, see below, we conclude that within the accuracy of our data our scaling procedure is justified.

The symmetry resolved ion yield curve measured by Hosaka *et al* [23] shows two local maxima in the σ channel. Of this, the second peak at 415 eV, which is the absolute maximum, is assigned to the shape resonance in both $^3\Pi$ and $^1\Pi$ channel, while the first peak at 412.5 eV is tentatively assigned to double excitations. In our light attenuation measurement the cross-section has less pronounced structures, which might be due to directional averaging. Agreement of our data to the older study by Lindle *et al* [21] is satisfactory.

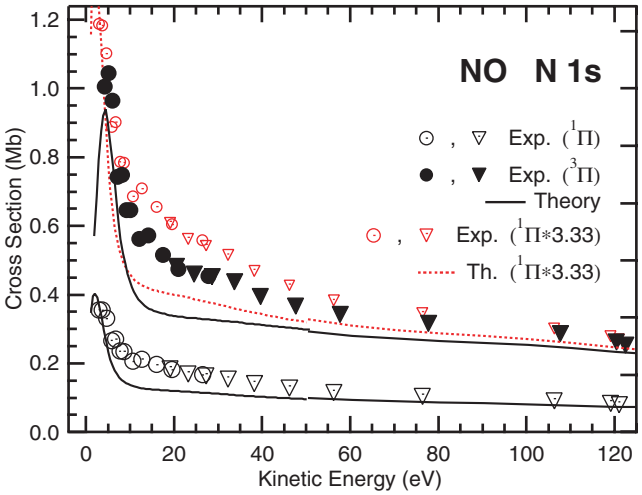

Figure 3. Partial photoionization cross-sections for the two NO N $1s^{-1}$ final states. Circles and triangles mark different experimental data sets. Experimental errors are about the symbol size. Theoretical results up to 50 eV include averaging over the vibrational motion, see text. Small symbols and the dotted line represent the $^1\Pi$ results, multiplied by 3.33 (see text).

The difference between the N 1s single-hole cross-section and the core-level photoabsorption cross-section has to be attributed to N 1s satellite production, of which no photon energy-dependent studies are known to the authors. Spears *et al* [50] find a total satellite intensity of 25% relative to the main line at the photon energy of the Al Kα line. If we use this number to partition the photoabsorption cross-section at 530 eV, the contribution of N 1s related shake-off processes is another 16% of the N 1s single-hole cross-section. A measurement of the total N 1s satellite intensity at 430.65 eV carried out within the scope of this work gives an intensity of discrete satellites of 35% relative to the sum of the main lines, which is in good agreement to the difference of the single-hole cross-section to the photoabsorption curve at this energy. (At this low energy, shake-off processes are unimportant.) No influence of the NO O 1s $\rightarrow \pi^*$ resonance on the N 1s cross-section can be seen.

We have disentangled the cross-section for ionization into the $^3\Pi$ and the $^1\Pi$ final states over a wide range of energies. Results are displayed in figure 3, together with the calculated curves. The cross-sections show an unusually steep decrease just above the photoionization threshold, as a consequence of the shape resonance embedded in the photoionization continuum at this photon energy. Early calculations within the multiple scattering model [51] placed the shape resonance somewhat higher at around 420 eV. In our calculations, the shape resonance positions are found at 413.2 and 415.2 eV for the $^1\Pi$ and $^3\Pi$ states, respectively. Due to the poor transmission of our analyser at low kinetic energies, we can only note from the experimental data that the $^3\Pi$ state most probably has a maximum in the cross-section at 415.4 eV. The shape resonances appear to be somewhat broader and the increase of the cross-section is less pronounced than in the calculation.

The intensity ratio of photoelectrons pertaining to different multiplet levels of an open-shell system has been examined for atomic oxygen by Schaphorst *et al* [52]. These authors distinguish between 'kinetic' and 'dynamic' effects. The kinetic effects are caused by the difference in

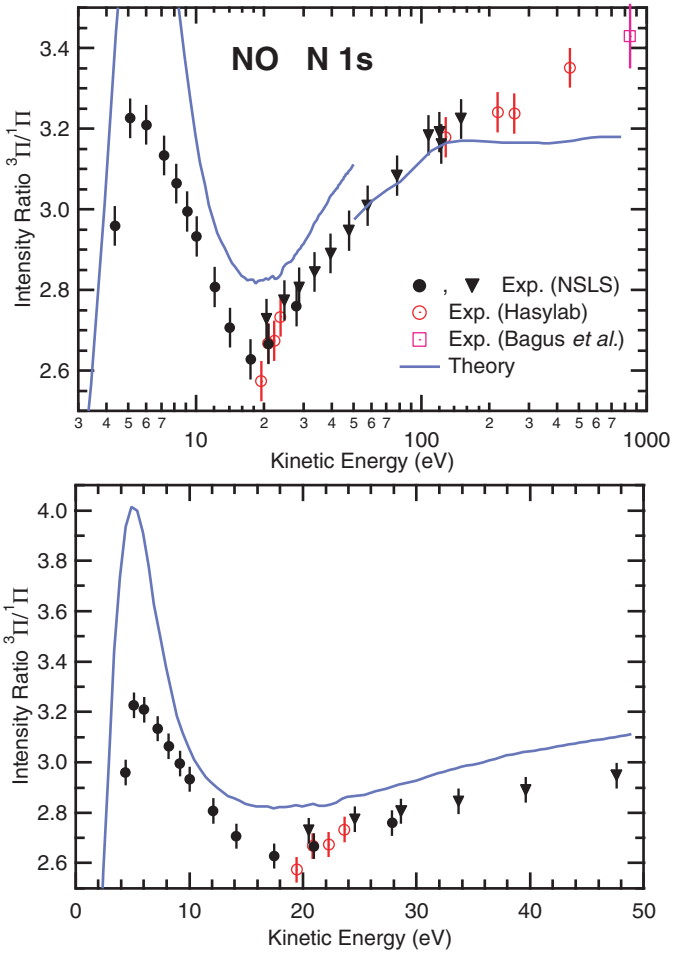

Figure 4. Intensity ratio of the two NO N $1s^{-1}$ photoelectron lines, above: wide energy range (note the log scale), below: expanded view of the region near threshold. Three experimental data sets (circles and triangles) and theory from this work (solid line) are shown. To perform the ratio of data points at equal kinetic energy, the original measurements at equal photon energy were interpolated linearly or by a polynomial fit. The value at 844 eV is from [19].

the ionization thresholds of the multiplet levels. If the cross-section ratio is performed at equal photon energies, this leads to variations even if the multiplet specific cross-sections versus kinetic energy only differ by degeneracy factors. In contrast, dynamic effects arise from a multiplet specific kinetic energy-dependent behaviour of the photoionization amplitudes. For the cross-section ratio of the oxygen $2s^12p^4$ (^{2,4}P) states, the variation was attributed solely to kinetic effects [52].

Figure 3 displays our data versus their respective kinetic energy. Significant differences between the cross-sections of the two channels exist between 10 and 50 eV kinetic energy. (To make this fact more evident, in the figure we have put in a copy of the $^1\Pi$ cross-section data multiplied by a factor to align them with the $^3\Pi$ cross-section at the high energy end of the figure.) In figure 4, the difference between the two channels is seen as a significant minimum in

the $^3\Pi/^1\Pi$ intensity ratio at around 20 eV kinetic energy. This observation clearly distinguishes the results from other photoionization experiments on closed- and open-shell systems.

5. Discussion: NO N 1s

To examine the source of the observed dynamic effect, consider the simple frozen core Hartree–Fock model given in [53]. For each final state of the ion+electron system, $^2\Pi$, $^2\Sigma^+$, $^2\Sigma^-$, $^2\Delta$, and each underlying ionic state, $^3\Pi$ or $^1\Pi$, a single-particle differential equation for the continuum orbital can be formulated. For the $^2\Pi$ final state, we get

$$\left(f + \sum_i (2J_i - K_i) + J_{2\sigma} + J_{2\pi} \pm \frac{K_{2\sigma}}{2} \pm \frac{K_{2\pi}}{2} - \varepsilon\right)\psi_{k\sigma} = 0. \tag{1}$$

Here, f contains all one-particle operators (kinetic energy and Coulomb attraction from the nuclei), J_k and K_k are the Coulomb and exchange operators with an electron in orbital k, i runs over all doubly occupied orbitals in the ionic state and ε is the single-particle energy of the continuum electron. The N 1s orbital is designated as 2σ. For the remaining final states, equations are similar and differ mainly in the symmetry of the continuum orbital. (Two additional terms, which pertain to Coulomb- and exchange-like interactions with the 2π valence orbital are present only for $^2\Sigma$ final states and will not be discussed here.) The important point in equation (1) is that it differentiates between the two ionic state symmetries by the 'sign of the exchange operators' $K_{2\sigma}$ and $K_{2\pi}$. In each case, these appear with the upper (positive) sign in the single-particle equations pertaining to the $^3\Pi$ ionic state and with a negative sign for the $^1\Pi$ ionic state. Since the exchange operators generally have a positive contribution to the potential, the triplet potential is less attractive than the singlet potential. This fact can also be seen from our numerical coupled-channel results: we find the shape resonances at photoelectron kinetic energies of 2.1 eV and 4.4 eV for $^1\Pi$ and $^3\Pi$ states, respectively. The fact that the resonances appear at different positions in each channel also shows that the amount of interchannel coupling is relatively small, in contrast to the valence ionization of NO [45]. Overall, the computed results shown in figure 3 indicate that the two-channel calculations given here show a difference in the $^1\Pi$ and $^3\Pi$ cross-sections comparable to that found in the experiments, although the calculations each disagree with the experimental results in a manner that suggests that the inclusion of shake-up channels will be important. Including these additional channels would more accurately represent the dynamic response of the target to the photoelectron and could thus change the position and the width of the shape resonance.

If we single out the exchange operators in equation (1), insert their definition and introduce a symbol $\hat{O}$ which summarizes the effect of all other operators, we have

$$\hat{O}\psi_{k\sigma}(\mathbf{r}) \pm \frac{\phi_{2\sigma}(\mathbf{r})}{2}\int \mathrm{d}\mathbf{r}'\,\frac{\phi^*_{2\sigma}(\mathbf{r}')\psi_{k\sigma}(\mathbf{r}')}{|\mathbf{r}-\mathbf{r}'|} \pm \frac{\phi_{2\pi}(\mathbf{r})}{2}\int \mathrm{d}\mathbf{r}'\,\frac{\phi^*_{2\pi}(\mathbf{r}')\psi_{k\sigma}(\mathbf{r}')}{|\mathbf{r}-\mathbf{r}'|} = \varepsilon\psi_{k\sigma}(\mathbf{r}) \tag{2}$$

and again we arrive at analogous equations for the other final-state symmetries. The negative signs again correspond to the $^1\Pi$ ionic state.

On the left-hand side (lhs) this equation contains the transformed continuum wavefunction, with contributions of bound state functions, multiplied by some exchange operators, added or subtracted. These latter contributions (last two terms on the lhs of the equation) differ from zero

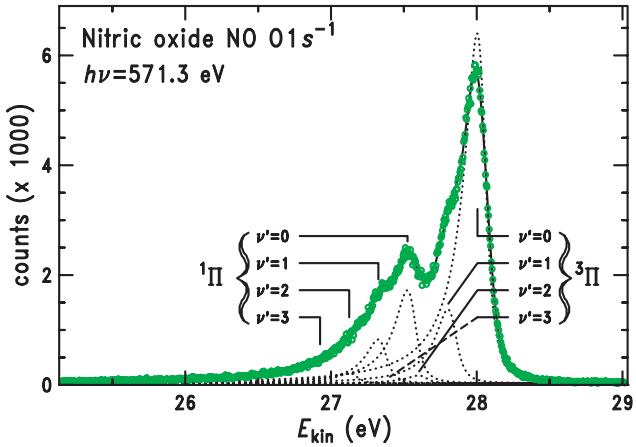

Figure 5. The NO O 1s main line photoelectron spectrum. The exchange split of the $^3\Pi$ and $^1\Pi$ states is much smaller than for the N 1s main line. Circles: experiment; solid line: least-squares fit; dashed lines: vibrational components of the fit, not convoluted with the apparatus function.

only in the molecular region. We expect the largest exchange terms to be the combination of the 2σ orbital with the σ continuum channel, since the former is strongly centred around the nitrogen core and will overlap with positive parts of the continuum wavefunction only. This contribution is 'positive' for the $^3\Pi$ and 'negative' for the $^1\Pi$ state. Since equation (2) is an eigenvalue equation, the latter contributions plus the continuum wavefunction transformed by the kinetic energy operator and the Coulomb attraction operator, summarized as $\hat{O}$, have to match the continuum wavefunction itself. For a given value of the kinetic energy ε, this is only possible if the effect of the kinetic energy and Coulomb attraction operators on the continuum orbital compensate the contributions of bound state character by the exchange terms. In order to achieve this, the continuum orbital of the $^1\Pi$ state, where the bound state terms are negative, needs to have 'more' charge density in the molecular region than the continuum orbital of the $^3\Pi$ state.

We suggest that this mechanism leads to the larger cross-section for the singlet channel at higher kinetic energies, where the shape resonance has little influence on the photoemission process. For the exchange terms with the 2π-bound orbital and with the π continuum channels, we expect lesser effects from this mechanism, since the wavefunctions are more extended and overlap in regions with matching and with opposite sign. Eventually, for very high kinetic energies, the continuum wavefunction oscillates rapidly in the molecular region. Thus, destructive interference of the continuum and bound state wavefunction will make the exchange integral insignificant.

6. Results: NO O 1s

The high resolution core-level photoelectron spectrum at the O 1s edge is shown in figure 5. The exchange splitting for the NO O $1s^{-1}$ states is much smaller than for the N $1s^{-1}$ states, 0.48 eV according to our measurements. This difference can be understood by inspecting the charge density of the singly occupied 2π orbital at the nitrogen and oxygen cores. Due to the higher electronegativity of the oxygen, the bonding 1π orbital is drawn towards the oxygen, so that the antibonding 2π electron is localized towards the nitrogen and thus interacts more strongly

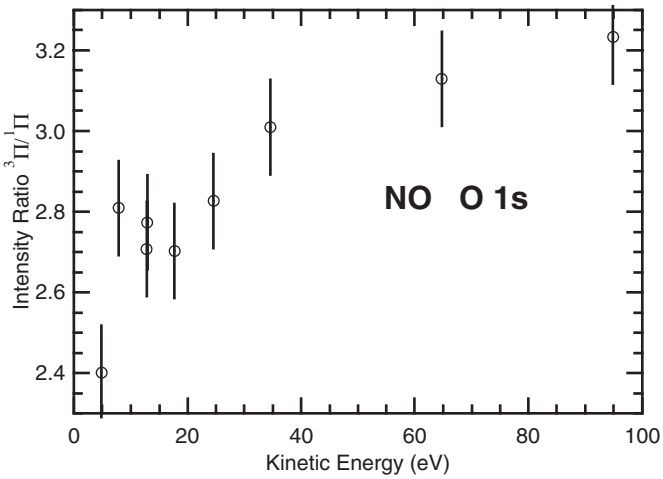

Figure 6. Intensity ratio of the two multiplet components of the NO O $1s^{-1}$ photoelectron line. The components were separated by a least-squares fit and ratios of the areas found in the fit were performed at equal photon energies.

with the N 1s orbital than with the O 1s orbital. Within this work, the vibrational spacing for both progressions was assumed to be equal and was found at a value of 200 meV. Unpublished work by one of the authors [54], indicates that the $^1\Pi$ progression in fact has a somewhat larger vibrational energy, but this does not influence the results further discussed in this publication.

The intensity ratio of the two multiplet components after O 1s photoionization is displayed in figure 6. Since the two components can only be separated by curve-fitting, the data analysis has a larger degree of uncertainty than in the N 1s case. We nevertheless see that the basic trend observed for the triplet/singlet ratio at the nitrogen edge is reproduced. This points to the universality of the dynamical origin for unequal multiplet components.

7. Concluding remarks

To summarize, we have seen significant differences in molecular photoionization channels which differ only by the spin coupling of the remaining open shells. This explicitly shows the effect of exchange interactions on the photoelectron continuum wavefunctions. Because of the difficulty of including the non-local exchange operators, often in first approximations to photoionization it has been neglected. This work gives an experimental example of the error introduced by that assumption.

A tentative explanation of the effects using properties of the respective wavefunctions has been given. We would finally like to mention again that the asymptotic value of the cross-section ratio is influenced by shake-up satellites borrowing intensity from both multiplet states [20]. It is conceivable that this intensity borrowing is photon energy dependent as well and would thus lead to some variation of the multiplet ratio at the highest photon energies we have discussed. This factor has not been considered here, since no energy-dependent measurements of the NO core-level satellite structure are known to the authors. For a further investigation of a possible relation between NO satellites and multiplet intensity, however, an investigation of the satellite structure at a number of energies seems to be indispensable.

Acknowledgments

Contributions of A T Wen and F Bernal to data acquisition are gratefully acknowledged. We thank S Hulbert for technical support at the NSLS. This work has been funded in part by the Deutsche Forschungsgemeinschaft and by the Fonds der chemischen Industrie. RRL and PL acknowledge support of the Welch Foundation (Houston) under Grant A-1020. The National Synchrotron Light Source is supported by the US Department of Energy, Division of Material Sciences and Division of Chemical Sciences.

References

[1] Einstein A 1905 *Ann. Phys., Lpz.* **17** 132
[2] Leahy D J, Reid K L and Zare R N 1991 *J. Chem. Phys.* **95** 1757–67
[3] Tsubouchi M, Whitaker B J, Wang L, Kohguchi H and Suzuki T 2001 *Phys. Rev. Lett.* **86** 4500–3
[4] Golovin A V 1991 *Opt. Spectrosc. (USSR)* **71** 537–41
[5] Shigemasa E, Adachi J, Oura M and Yagishita A 1995 *Phys. Rev. Lett.* **74** 359–62
[6] Watanabe N, Adachi J, Soejima K, Shigemasa E, Yagishita A, Fominykh N G and Pavlychev A A 1997 *Phys. Rev. Lett.* **78** 4910–3
[7] Golovin A V, Heiser F, Quayle C J K, Morin P, Simon M, Geßner O, Guyon P M and Becker U 1997 *Phys. Rev. Lett.* **79** 4554–7
[8] Heiser F, Geßner O, Viefhaus J, Wieliczek K, Hentges R and Becker U 1997 *Phys. Rev. Lett.* **79** 2435–7
[9] Davies J A, Continetti R E, Chandler D W and Hayden C C 2000 *Phys. Rev. Lett.* **84** 5983–6
[10] Landers A *et al* 2001 *Phys. Rev. Lett.* **87** 013002
[11] Jahnke T *et al* 2002 *Phys. Rev. Lett.* **88** 073002
[12] Gessner O, Hikosaka Y, Zimmermann B, Hempelmann A, Lucchese R R, Eland J H D, Guyon P M and Becker U 2002 *Phys. Rev. Lett.* **88** 193002
[13] Kugeler O, Prümper G, Hentges R, Viefhaus J, Rolles D, Becker U, Marburger S and Hergenhahn U 2004 *Phys. Rev. Lett.* **93** 033002
[14] Saito N *et al* 2004 *Phys. Rev.* A **70** 062724
[15] Reid K L, Leahy D J and Zare R N 1991 *J. Chem. Phys.* **95** 1746–56
[16] Reid K L, Leahy D J and Zare R N 1992 *Phys. Rev. Lett.* **68** 3527–30
[17] Ito K, Adachi J, Hikosaka Y, Motoki S, Soejima K, Yagishita A, Raseev G and Cherepkov N A 2000 *Phys. Rev. Lett.* **85** 46–9
[18] Motoki S, Adachi J, Ito K, Ishii K, Soejima K, Yagishita A, Semenov S K and Cherepkov N A 2002 *Phys. Rev. Lett.* **88** 063003
[19] Bagus P S, Schrenk M, Davis D W and Shirley D A 1974 *Phys. Rev.* A **9** 1090–6
[20] Darko T, Hillier I H and Kendrick J 1977 *Chem. Phys. Lett.* **45** 188–90
[21] Lindle D W, Truesdale C M, Kobrin P H, Ferrett T A, Heimann P A, Becker U, Kerkhoff H G and Shirley D A 1984 *J. Chem. Phys.* **81** 5375–8
[22] Kosugi N, Adachi J-I, Shigemasa E and Yagishita A 1992 *J. Chem. Phys.* **97** 8842
[23] Hosaka K, Adachi J, Takahashi M and Yagishita A 2003 *J. Phys. B: At. Mol. Opt. Phys.* **36** 4617–29
[24] Hosaka K, Adachi J, Takahashi M, Yagishita A, Lin P and Lucchese R R 2004 *J. Phys. B: At. Mol. Opt. Phys.* **37** L49–L55
[25] Randall K J, Feldhaus J, Erlebach W, Bradshaw A M, Eberhardt W, Xu Z, Ma Y and Johnson P D 1992 *Rev. Sci. Instrum.* **63** 1367–70
[26] Feldhaus J, Erlebach W, Kilcoyne A L D, Randall K J and Schmidbauer M 1992 *Rev. Sci. Instrum.* **63** 1454–7
[27] Kivimäki A, Hergenhahn U, Kempgens B, Hentges R, Piancastelli M N, Maier K, Rüdel A, Tulkki J J and Bradshaw A M 2001 *Phys. Rev.* A **63** 012716
[28] Köppe H M 1995 *PhD Thesis* Technische Universität, Berlin

[29] Hemmers O, Whitfield S B, Glans P, Wang H, Lindle D W, Wehlitz R and Sellin I A 1998 *Rev. Sci. Instrum.* **69** 3809–17
[30] Björneholm O, Federmann F, Larsson C, Hahn U, Rieck A, Kakar S, Möller T, Beutler A and Fössing F 1995 *Rev. Sci. Instrum.* **66** 1732–4
[31] Moddeman W E, Carlson T A, Krause M O, Pullen B P, Bull W E and Schweitzer G K 1971 *J. Chem. Phys.* **33** 2317–36
[32] Remmers G, Domke M, Puschmann A, Mandel T, Kaindl G, Hudson E and Shirley D A 1993 *Chem. Phys. Lett.* **214** 241–9
[33] Senf F *et al* 2001 *Nucl. Instrum. Methods* A **467** 474–8
[34] Mårtensson N, Baltzer P, Brühwiler P A, Forsell J-O, Nilsson A, Stenborg A and Wannberg B 1994 *J. Electron Spectrosc. Relat. Phenom.* **70** 117–28
[35] Baltzer P, Karlsson L, Lundqvist M and Wannberg B 1993 *Rev. Sci. Instrum.* **64** 2179–89
[36] Sodhi R N S and Brion C E 1984 *J. Electron Spectrosc. Relat. Phenom.* **34** 363–72
[37] Kuchiev M Y and Sheinerman S A 1986 *Sov. Phys.—JETP* **63** 986–90
[38] Armen G B, Tulkki J, Åberg T and Crasemann B 1987 *Phys. Rev.* A **36** 5606–14
[39] Hergenhahn U 2004 *J. Phys. B: At. Mol. Opt. Phys.* **37** R89–R135
[40] Köppe H M, Kilcoyne A L D, Feldhaus J and Bradshaw A M 1995 *J. Electron Spectrosc. Relat. Phenom.* **75** 97–108
[41] Kempgens B, Itchkawitz B S, Erlebach W, Köppe H M, Feldhaus J and Bradshaw A M, unpublished work
[42] Itchkawitz B S, Kempgens B, Köppe H M, Feldhaus J, Bradshaw A M and Peatman W B 1995 *Rev. Sci. Instrum.* **66** 1531–3
[43] Stratmann R E and Lucchese R R 1995 *J. Chem. Phys.* **102** 8493–505
[44] Stratmann R E, Bandarage G and Lucchese R R 1995 *Phys. Rev.* A **51** 3756-65R
[45] Stratmann R E, Zurales R W and Lucchese R R 1996 *J. Chem. Phys.* **104** 8989–9000 and references therein
[46] Huber K P and Herzberg G 2005 *Constants of Diatomic Molecules* (data prepared by J W Gallagher and R D Johnson III) in NIST Chemistry WebBook, NIST Standard Reference Database Number 69, ed P J Linstrom and W G Mallard (Gaithersburg, MD: National Institute of Standards and Technology) http://webbook.nist.gov
[47] Müller J, Ågren H and Goscinski O 1979 *Chem. Phys.* **38** 349–359
[48] Rüdel A 2001 *PhD Thesis* Technische Universität, Berlin, p 91
[49] Chen H W, Jolly W L, Xiang S-F and Legzdins P 1981 *Inorg. Chem.* **20** 1779–82
[50] Spears D P, Fischbeck H J and Carlson T A 1975 *J. Electron Spectrosc. Relat. Phenom.* **6** 411–20
[51] Wallace S, Dill D and Dehmer J L 1982 *J. Chem. Phys.* **76** 1217–22
[52] Schaphorst S J, Krause M O, Caldwell C D, Saha H P, Pahler M and Jiménez-Mier J 1995 *Phys. Rev.* A **52** 4656–64
[53] Smith M E, McKoy V and Lucchese R R 1985 *J. Chem. Phys.* **82** 4147–54
[54] Hergenhahn U *et al* unpublished work